CONSIDERATIONS OF THE INFLUENCE OF PROCESS PARAMETERS ON THE MICROSTRUCTURE AND MECHANICAL PROPERTIES OF FRICTION STIR PROCESSED AL ALLOYS

Emilia Dobrin [1], Lia-Nicoleta Boțilă [2] and Gabriela-Victoria Mnerie [3]
[1] National R&D Institute for Welding and Material Testing - ISIM Timisoara, 30 Mihai Viteazu Blv, edobrin@isim.ro
[2] National R&D Institute for Welding and Material Testing - ISIM Timisoara, 30 Mihai Viteazu Blv, lbotila@isim.ro
[3] National R&D Institute for Welding and Material Testing - ISIM Timisoara, 30 Mihai Viteazu Blv, gmnerie@isim.ro

ABSTRACT: Aluminium alloys are widely employed across numerous thanks to their superior combination of strength, lightweight characteristics and corrosion resistance. In recent years, Friction stir processing (FSP) has come up as a promising technique for machining aluminium alloys, enabling greater control over microstructural evolution and mechanical properties. This paper provides an in-depth exploration the impact of process parameters on the microstructure and mechanical properties of aluminium alloys processed by FSP. The study focuses on the systematic investigation of the influence of the principle process parameters, including rotational speed, machining speed and applied pressure, on the microstructure and resulting mechanical performance of FSP machined aluminium alloys.
Furthermore, the mechanical properties of FSP treated aluminium alloys are measured by a comprehensive set of tests, including tensile tests, hardness measurements and fracture tests. The relationship between process parameters and the mechanical behaviour of the alloys is analysed in detail to identify the optimum conditions for achieving the desired properties.
Findings show that process parameters plays a significant role in defining the microstructure and mechanical properties of alloys.
KEYWORDS: aluminium alloys, cooling medium (air, underwater, cryogenic)

1. INTRODUCTION

FSW, an advanced form of friction welding, was initiated by TWI „The Welding Institute" in 1991 and has since become a leading metal joining technique. Initially used for aluminium alloys, FSW has expanded its applications a vast selection of metallic materials and even plastics.

FSW „Friction Stir Welding" is a solid state welding technique that has earned considerable attention in the industrial and research applications due to its unique advantages [1].

The FSW process involves a specialized tool with a shoulder and a profiled pin that is introduced between two base materials. The tool generates heat through friction and plastic deformation, facilitating material softening and bonding, as it can be seen in figure 1. The tool's rotation and translation cause material stirring and flow, leading to the formation of a solid state bond between the joined plates. The asymmetry in motion and heat transfer between advancing and receding part during FSW results in unique material flow patterns and joint formation [2].

In summary, FSW simulation and modelling plays a key function in optimizing process parameters, understanding material behaviour, and predicting the outcomes of the welding process, making it a valuable tool for engineers, manufacturers, and researchers in various industries.

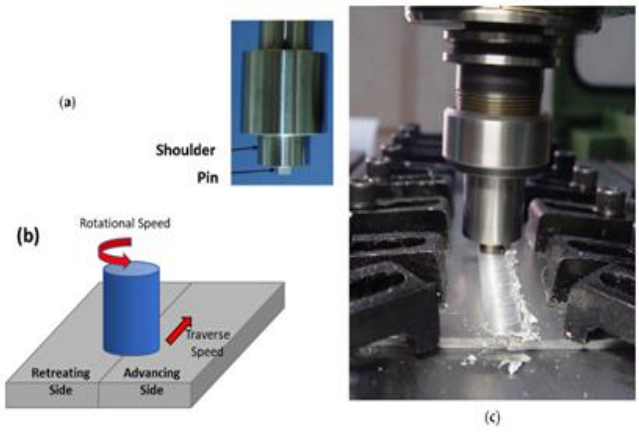

Figure 1. (a) a typical basic FSW tool, (b) a workflow diagram of the FSW process, and (c) a diagram of the FSW set-up [2]

FSP has been developed according to FSW is utilized to change metallic microstructures. Although the foundations and parameters of FSP and FSW are similar, there are minor differences between the two processes. However, in regard to microstructural changes and properties of material, there are no visible difference between them [3].

FSP involves a rotating tool pin that is inserted into the workpiece to induce localized modifications in the microstructure, leading to enhanced material properties. Unlike FSW, the primary objective of FSP is not to join two parts but to alter the material's structure. This technique enables the enhancement of strength, modification of microstructure, and attainment of a uniform distribution of the grain size. Moreover, FSP can adjust sediment distribution and

facilitate the production of surface composites [4]. Its applications span various areas, including the production of surface composites, homogenization of parts from powder metallurgy, modification of microstructures in metal-based composites, and enhancement of properties in cast alloys [5].

FSP has found applications across various materials such as aluminium alloys, magnesium alloys, and steels to enhance their properties and performance. Industries like aerospace, automotive, and marine utilize FSP to improve material characteristics.

One of the important advantages of FSP lies in its unique characteristics and capabilities. FSP revolutionizes the way materials are processed and offers several key aspects that make it a highly advantageous technique:

- FSP is a surface engineering approach employing a rotating tool to stir and blend the material surface without inducing melting. This method aids in achieving fine-grained structures uniformly throughout the thickness of the material;
- FSP is recognized for its capability to refine the grain structure of materials, resulting in improved mechanical properties like strength and ductility. It can create ultrafine-grained structures in a variety of alloys;
- Superplasticity: Materials treated with FSP exhibit superplastic behaviour, enabling significant deformation without fracturing. This characteristic is advantageous for shaping intricate forms and achieving high elongation;
- Control Parameters: significant parameters such as tool rotation speed, feed rate, tilt angle and cooling medium strongly determine the microstructure and properties processed material;
- Surface Integrity: FSP enhances the surface integrity of materials by eliminating flaws and establishing a uniform microstructure. This enhancement contributes to properties like corrosion resistance [6].

2. MATERIALS ANALYSED - ALUMINIUM ALLOYS

In contemporary manufacturing and technology sectors such as automotive and aerospace, aluminium and its alloys play a major role [7]. Industries are continuously pushing boundaries in aluminium alloy strength, damage tolerance and corrosion resistance to create durable and lasting alloys for diverse applications, thereby enhancing overall efficiency [8, 9].

AA2014 is an aluminium alloy known for its heat-treatable properties and high strength, attributed to the addition of copper as a major alloying element. Widely utilized in aeronautical and various industries due to favourable strength-to-weight ratio, AA2014 exhibits increased susceptibility to both pitting and intergrain corrosion in comparison with other aluminium alloys [10].

2A14 Al is similar to the AA2014 alloy but exhibits slightly higher tensile strength. Additionally, the alloy demonstrates corrosion resistance, making it a favourable choice for applications in harsh environments. Is a representative Al-Cu-Si-Mg forged aluminium alloy renowned for its exceptional strength, heat resistance, and excellent thermoplasticity. It finds extensive application in the manufacturing of forged and drop-forged components that experience significant loads. Additionally, 2A14 aluminium alloy is classified as a heat-treatable alloy, allowing for further enhancement of its mechanical properties through heat treatment. Among the various heat treatment methods available, the solution and artificial aging processes, commonly referred to as T6 treatment, are particularly effective in maximizing the alloy's strength [11, 12].

The **aluminium alloy 3xxx**: The Al-Si based alloys have gained significant popularity in the automotive industry as a substitute for cast iron in modern automotive powertrain manufacturing. This is primarily due to their advantageous combination of excellent strength-to-weight ratio and moldability. Among the die-cast aluminium alloys used in the automotive sector, the most prevalent ones include A356 and 319.

A319 This alloy exhibits excellent melding and machining characteristics. It shows high corrosion resistance, satisfactory weldability and mechanical properties. The anodized colour is normally grey with a brown tinge, influenced by the silicon and copper components. Popular applications for 319.0 sand castings include a wide variety of structural castings for engine components, gas and oil tanks, and general industrial commercial uses. However, it is important to remember that the A319 type alloys have a relatively smaller strength at room temperature, which is considered their main drawback.

A356 shows exceptional casting and machining characteristics. It boasts excellent corrosion resistance and very satisfactory weldability. The mechanical properties are reported to be excellent. Typical uses for this alloy may include aircraft castings, pump casings, impellers, high-speed blowers, and structural castings where high strength is required. Its favourable moldability makes it an excellent choice for difficult and complex castings

demanding lightweight properties, pressure tightness and superior mechanical performance [13, 14].

AA5083: The aluminium alloy 5xxx series is extensively used in marine applications, particularly for ship hulls. It is one of the most prominent members of the 5xxx series, with numerous applications in aircraft, marine structural components, and automobiles [15]. Welding aluminium alloys is crucial for constructing structural frameworks and mechanical fabrications, including aircraft and marine vessels. However, welding can be problematic and often poses significant challenges. Common welding defects in aluminium include incomplete fusion, hot cracking, and porosity [16].

AA5083-H111: The prevalent tempers for 5083 aluminium include: H111 - Exhibiting some work hardening from shaping processes, though not to the extent required for the H11 temper, O - Soft and H32 - Undergoing work hardening through rolling, followed by stabilization via low-temperature heat treatment to attain a quarter-hard state [17].

AA7075 aluminium alloy is widely used for several high-technology applications such as: the aeronautical, marine, automotive and defence sectors due to superior strength to weight ratio. The 7075 aluminium alloy series stands out due to its exceptional strength, comparable to that of many steels. This high strength is one of its most attractive characteristics, but it is the combination with its other properties that make it an ideal choice for structural parts subjected to high stress. Notably, it possesses a low density, excellent machinability, and remarkable corrosion resistance. While its corrosion resistance is relatively lower than some other aluminium alloys, it still outperforms many of the 2000 series alloys in this regard. In applications where mechanical properties are of utmost importance, the use of 7075 aluminium often compared that of 2014. However, when higher mechanical properties are required, 7075 remains the preferred choice [18].

The materials previously discussed have undergone various studies and research to evaluate the potential of the FSP process in different environments: ambient atmosphere, liquid medium, and frozen conditions. These studies focused on welded joints made from these materials, examining both similar and dissimilar material pairs. The chemical composition and mechanical properties of the metallic materials investigated in this study are detailed in Tables 1 and 2, respectively.

Table 1. Chemical composition of the presented materials [12, 19, 21 - 23]

Material type	Mg	Zn	Ti	Cr	Si	Mn	Fe	Cu	Al
AA2014	0.80	0.17	0.02	0.03	0.69	0.64	0.23	4.26	Bal.
2A14 Al	0.88	-	0.02	-	0.08	0.96	0.02	0.46	Bal.
2A14-T4	0.4 - 0.8	0.3	0.15	-	0.6-1.2	0.4-1	0.7	3.9 - 4.8	Bal.
A319	0.291	0.465	0.163	0.01	6.52	0.459	0.435	3.88	-
A356	0.05	-	0.12	-	6.65	0.03	0.07	0.05	Bal.
AA5083	4.6	0.009	0.027	0.1	0.14	0.63	0.3	0.018	Bal.
AA5083-H111	4.254	0.08	0.01	0.09	0.980	0.52	0.259	0.346	94.42
AA7075	2.1 - 2.9	5 - 6	-	-	0.5%	-	-	-	87.1 - 91.4

Table 2. Mechanical properties of parent materials [12, 23 - 27]

Material type	Tensile strength (MPa)	Yield strength (MPa)	Elongation (%)	Microhardness (HV)
AA2014	483	310	14	150
2A14 Al	490	320	12	-
2A14-T4	424	-	15 - 17	120 - 125
A319	235 - 280	130 - 185	2.5 - 3	74 - 114
A356	164 - 265	124 - 185	6 - 50	61 - 94
AA5083	315	225	15	95
AA5083-H111	275	270	10	65
AA7075	560	480	7.9	150

3. INFLUENCES OF PARAMETERS ON MECHANICAL PROPERTIES

In the course of experimental studies and research on FSP processing of aluminium alloy welds presented in Table 1, processing tools made of various metallic materials with different geometrical configurations were utilized (Table 3) plus process parameters used in welding and processing.

Table 3. Processing tools data and process parameters used in welding and processing

Base material	Shape/material of work tool	Welding parameters FSW	Process parameters FSP/ SFSP/ CCFSP (cryogenic cooled FSP)
Similar plates of **AA2014** Dimensions = 280 x 120 x 4 mm	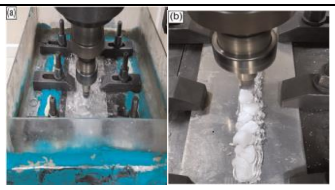 high carbon steel (H13) with cylindrical spiral pin, shoulder diameter = 24 mm pin length Lpin = 3.8 mm pin diameter Øpin = 8 (top) and 6 (bottom) mm	**FSW/SSFSW [28]** -Rotational speed: 1100 rpm, -Welding speed: 30 mm/min, -Tilt angle: 2^0 - SSFSW „Stationary shoulder friction stir welding" is a technology where the rotation speed of the stirring pin was configured to various values	**FSP, SFSP, CCFSP (cryogenic cooled FSP)** for the same set of parameters FSP in air, underwater, and dry ice [28] are: - Tool processing speed: 1100 rpm; - Travelling speed: 30 mm/min.
AA 2024, two plates 3.5 mm thick. It is uses Al_2O_3 nanoparticles as reinforcement particles.	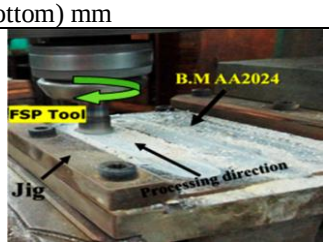 - tool: cylindrical shape hardened K-110 steel; - shoulder diameter= 25 mm; - pin diameter Øpin = 8 mm; - pin length Lpin = 2.5 mm.	**FSW [29]** - Rotational speed: 800 rpm; - Welding speed: 50 mm/min.	**FSP [30]** - The alloy plates were grooved to 3 mm wide and 2 mm deep mm prior to FSP application; -Tool processing speed were carried out for: 900, 1120, 1400, and 1800 rpm; - Three travel speeds at: 10, 15, and 20 mm/min; - tool tilt angle: 2^0; - tool plunge speed: 0.5 mm/s; - dwell time: 2 s -no. of multi-passes = 3.
2A14 Al, with homogenized plates with dimensions 220 × 60 × 6 mm	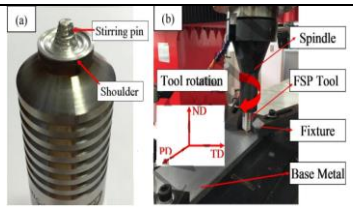 pin length Lpin= 5 mm pin diameter Øpin= 6 (top), 4 mm (bottom) shoulder diameter Ø=15 mm	**FSW [5]** -Welding speed:120 mm min^{-1} - Welding speed: 1000 rpm - Before FSP the plates were submitted to homogenization process that consists of heating to 490^0C for 10 h [29].	**FSP [5]** -no. of passes FSP = 1 were conducted with a back - tilt angle: 2.5 °; -Traverse speed-120 mm min^{-1} - Processing speed-1000 rpm; -The initial temperature of cooling medium for air, ambient water, ice water and dry ice is 25°C, 25°C, 2°C and -20°C [29].
6.35 mm thick **AA2014-T6** alloy plates with composite surface reinforced with SiC particles in AA2014 alloy.	- hot die tool: 50 HRC; - pin length Lpin = 3 mm - pin diameter Øpin = 5 (top) and 3 mm (bottom); - shoulder diameter Ø = 21 mm.	**FSW [31]** - Rotation speed: 710 rpm; -Welding speed: 100 mm/min.	**FSP [31]** - After packing the groove, four passes of FSP were applied with 100% overlap using clockwise tool rotation. - Tool processing speed: 710 rpm; - Traverse speed: 100 mm/min.
Dissimilar material overlapped **A319xA356** with dimensions -16 mm x 50 mm x 200 mm	Pin tool: cylindrical hemispherical tip - pin diameter Øpin = 5.2 mm - shoulder diameter Ø = 13 mm - pin length Lpin = 3.4 mm	**FSW [32]** - Rotation speed: 1000 rpm - Welding speed: 1.7 mm/s [31].	**Multi- FSP A319 [32]** -Tool processing speed: 1000 rpm, -Translation speed: 1.7 mm/s, - no. of passes = 1 for length = 150 mm. - no. of passes = 5 - 6, on intervals of about 4 mm.
Cu-Reinforced AA5083	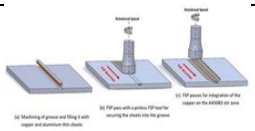 Pin tool – cylindrical, right-handed thread - pin diameter Øpin = 4 mm - pin length Lpin = 4 mm - flat shoulder diameter Ø = 22 mm [32].	**FSW [6]** - Rotation speed: 1000 rpm - Welding speed: 13 mm/min	**FSP [6]** - Processing speed: 1000 rpm; -Transverse speed: 13 mm/min.

Similar plates from **AA5083** Dimensions=120 mm × 100 mm × 6 mm	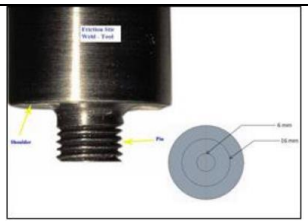 - pin length-5.70 mm, - pin diameter-6 mm, - tool shoulder-16 mm - shank-40 mm	**FSW [32]** - Rotation speed: 600 rpm -Welding speed: 85 mm/min -Tool tilt angle = 1^0	**FSP [32]** -Processing speed, 600/750/900 rpm; -Welding speed; 70/85/100 mm/min - Angle of inclination of the tool = 0, 1, 2 (Ɵ)
Similar plates of **AA-5083-H111** dimensions=90 × 10 × 3mm	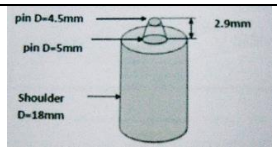 Pin tool - taper cylindrical Made of x 38 steel	**FSW [33]** - Rotation speed: 1500 rpm - Welding speed: 20mm/min	**FSP [33]** -Processing speed: 1500rpm -Travel speed: 40 mm/min
Al7075 with dimensions of 10 × 10cm and the thickness of 10mm.	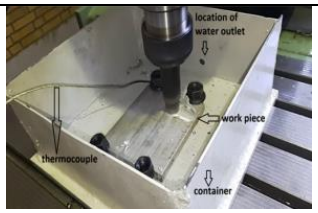 pin length: 18 mm, pin diameter: 5 mm, tool shoulder: 8 mm	**FSW [34]** - Rotation speed: 1250rpm - Welding speed: 63 mm/min.	**FSP/SFSP [34]** **FSP:** - Processing speed: 1250rpm - Travel speed: 63 mm/min. **SFSP:** - Processing speed: 1250rpm - Travel speed: 43 mm/min water temperature remained stable at 30◦C

Based on the microstructural characterization analysis of two similar **AA2014** plates using FSP under different cooling conditions (air cooled, dry ice cooled and under water) as shown in the figure 2, the following results were obtained:

- During FSP, the working metal experiences SPD „severe plastic deformation" and DRX „dynamic re-crystallization";
- The size of the grains in the stir zone of various cooling conditions (ambiental air, dry ice, and underwater) for AA2014 was observed to be 4.9 mm, 3.5 mm, and 0.9 mm, respectively;
- It was noted that the fractions of high-angle boundaries were bigger in the underwater FSP sample in comparison to other conditions for AA2014;
- The ultra fine-grained microstructure (0.9 mm grain size) obtained in the underwater FSP for AA2014 was assigned to the uniform heat dispersion in water, which lead to improved mechanical properties such as hardness and resistance in comparison to different conditions [27].
- The choice of cooling medium during FSP has a great influence on the mechanical properties of AA2014 alloy2014 samples. While air cooling may result in lower hardness and strength, water cooling enhances these properties by promoting finer grain structures [27]. For the AA2014/SiC surface composite, the hardness of the base alloy decreased after FSP, but the surface composite exhibited an increase in hardness due to the incorporation of harder ceramic particles. The selection of the cooling medium during FSP significantly affects the mechanical properties of AA2014 alloy samples. While air cooling may lead to lower hardness and strength, water cooling enhances these properties through finer grain structures [27].

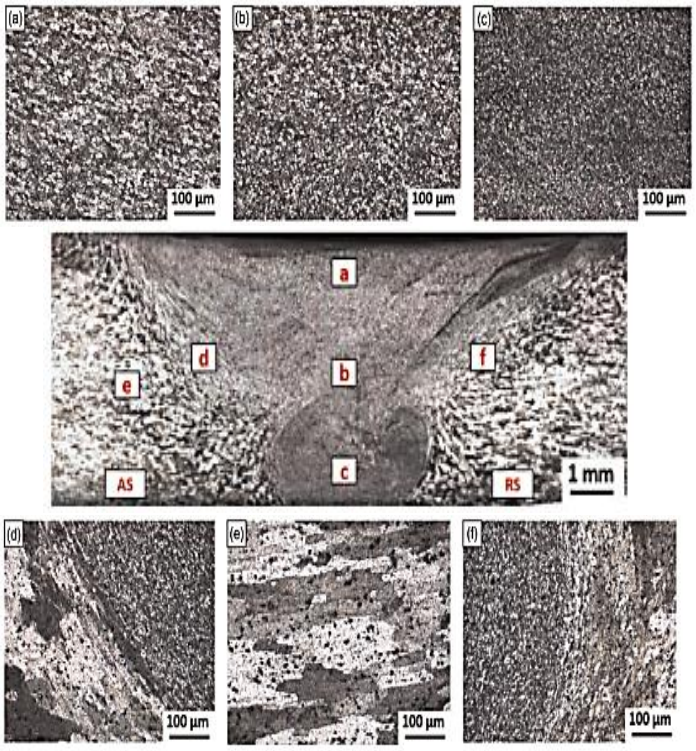

Figure 2. Microstructures of (a) TSZ, (b) MSZ, (c) BSZ, (d) AS-TMAZ, (e) HAZ, (f) RS-TMAZ of ACFSP specimen along with macrostructure. AS: advancing side; RS: retreating side; TMAZ: thermo-mechanically affected zone; HAZ: heat-affected zone; TSZ: top portion of the stir zone; MSZ: middle portion of the stir zone; BSZ: bottom portion of the stir zone [27]

In the case of the **AA2014/SiC** surface composite, the hardness of the base alloy decreased after FSP, but the surface composite showed an increase in hardness due to the incorporation of harder ceramic particles.

The surface composite hardness was observed to be 150 HV as depicted in figure 3, nearly twice that of the FSPed base alloy, indicating the positive impact of SiC reinforcement on hardness.

The hardness of the stir zone in the surface composite increased from 63 to 96 HV because of the existence of SiC particles and grain refinement [28].

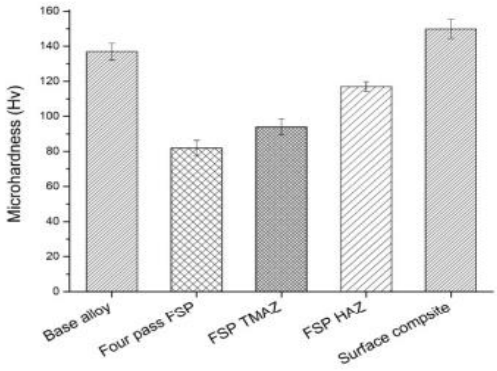

Figure 3. Hardness of base alloy, FSPed alloy and surface composite [28]

For the two plates of AA2024 reinforcerd with Al_2O_3 nanoparticles, tool rotation speed is found as a relevant process variable in FSP, which affects material temperature, mixing action and nanoparticle distribution. There are four rotation speeds (900, 1120, 1400 and 1800 rpm) and three linear speeds (10, 15, and 20 mm/min) were examined. Tensile strength improvements were observed with increasing rotational speed up to a given limit as shown in graphs 4 and 5. The multi-pass FSP technique was found to refine grain size and enhance mechanical properties, particularly tensile strength, by 25% compared to the basic metal.

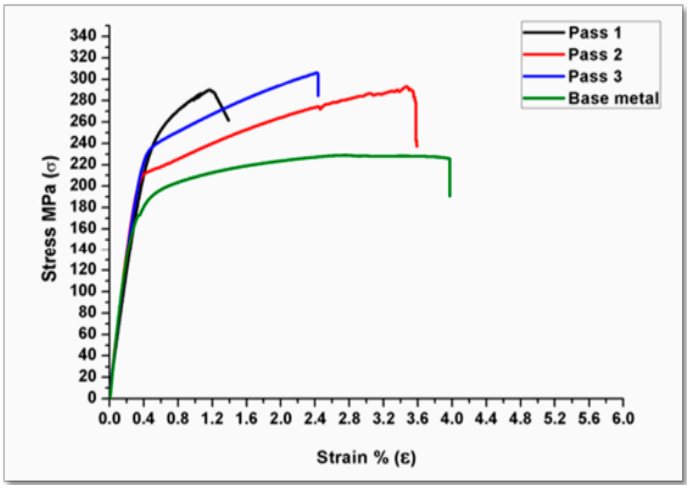

Figure 4. The representations of pass number on tensile strength at a rotational speed of 1800 rpm for a travel speed of 15 mm/min [30]

The addition of Al_2O_3 nanoparticles as reinforcement enhanced the composite's performance, with the particles being well-distributed within the matrix. However, it was observed that a single pass was insufficient to fully optimize the mechanical properties due to residual voids or defects. These results are consistent with previous studies and indicate a trade-off between increased strength and potentially reduced ductility in metal matrix composites [30].

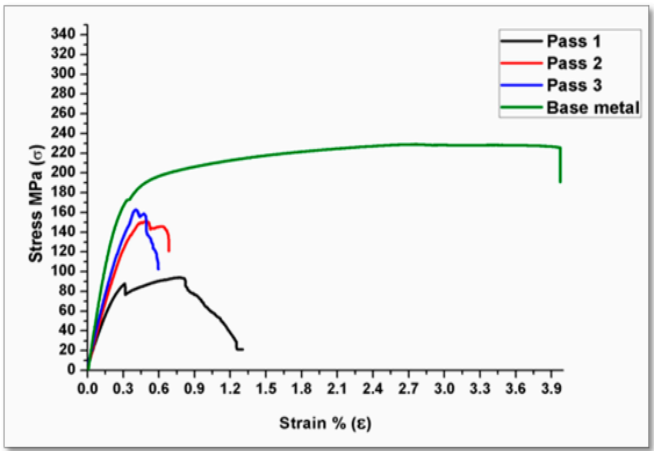

Figure 5. The graphics of pass number on tensile strength at 1800 rpm for a 15 mm/min travel speed. [30]

The fracture toughness graphs are presented in a comparative manner, depicting the impact of rotational speed on the toughness at variable numbers of passes. In figure 6, the impact of rotational speed on ultimate tensile strength is reported. It is shown that the rotational speeds of 900 rpm and 1120 rpm result in higher ultimate tensile strength in comparison to other speeds, in particular, when processed at travel speeds of 10 mm/min and 14 mm/min. In general, the inclusion of a third pass induces an improvement in tensile strength, with the maximum value improved by 27% relative to the base metal. However, when the rotational speed of the tool is set at 1800 rpm, a much lower ultimate tensile strength is obtained over the three passes.

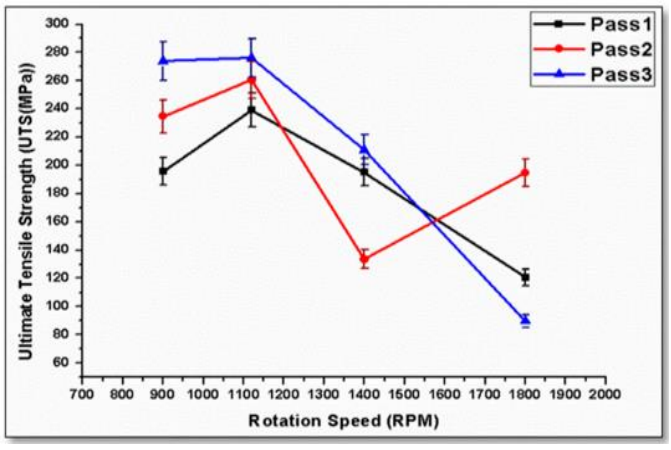

Figure 6. The effect of rotational speed on ultimate tensile strength at a travel speed of 10 mm/min for three passes [30]

FSP brings about notable alterations in the microstructures of **A319** and **A356** cast dissimilar material bars. These changes encompass refinement, eradication of dendritic structures, decrease in porosity, uniform dispersion of particles, and enhancements in hardness distribution. These microstructural adjustments are essential in increasing the mechanical properties of the alloys and elevating their overall performance.

The processed alloys exhibited higher ultimate tensile strengths compared to their as-cast counterparts, indicating an improvement in the material's ability to withstand maximum tensile stress. The tests results indicate that FSP processing led to significant improvements in both ultimate tensile strengths and ductility of A319 and A356 cast bars. These enhancements play an important role in enhancing the overall performance and reliability of the alloys across diverse applications [31].

In the case of plates from the non-heat treatable aluminium alloy **AA5083-H111** served as the base material, while pure copper was employed as the reinforcing material. Reinforcements were integrated into the aluminium matrix through in-situ chemical reactions between copper and AA5083 during the FSP process. Copper was chosen due to its relatively high solubility in aluminium, and the Al-Cu system is under extensive investigation for its potential applications across a range of temperatures.

FSW-welded joints of **Cu-reinforced AA5083** were subjected to multiple processing by FSP. Macrographs of Cu-reinforced aluminium alloy cross-sections after FSP processing are examined. Dark regions denote unincorporated copper in the AA5083 stir zone. In particular, unincorporated copper decreases with successive FSP passes. In single-pass specimens, there are noticeable copper zones in the upper region of the stir zone. At two passes, this decreases, and small copper-based particles are formed due to diffusion, generating intermetallic layers. In the case of three-pass specimens, unincorporated copper is confined to small regions of the upper stir zone, while numerous fine copper-based particles are evenly distributed throughout the zone. The FSP three-pass specimen was chosen for further microstructural analysis [6].

Integration occurred primarily in the form of copper-based intermetallic particles and, secondarily, through copper diffusion into the AA5083 matrix. Microstructural analysis revealed that the copper-based particles comprised layers with varying stoichiometric compositions. At the core of these particles, particularly those with diameters ranging from 30 to 80 μm, pure copper was observed.

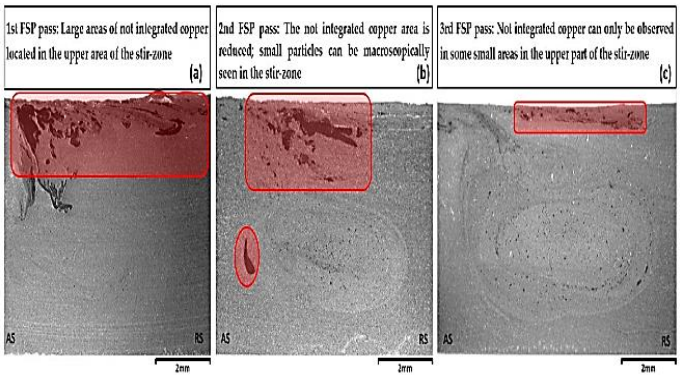

Figure 7. Macrographs of the cross-sections of Cu-reinforced FSPed 5083-H111 specimens with: (a) one FSP pass, (b) two FSP passes, and (c) three FSP passes [6]

The macrohardness distribution within the copper-reinforced mixing zone significantly increased from 77 HV to 138 HV.

The significant increase in macrohardness values in the mixing zone, compared to the FSP-ed sample without copper addition, is primarily due to the high concentration of Al-Cu intermetallic compounds and, secondarily, to the diffusion of copper into the AA5083 matrix [6].

Microstructural analysis of FSW welding of two similar AA5083 materials, processed by FSP, revealed that the intense plastic deformation and recrystallization during FSP resulted in a finer and more uniform grain size distribution compared to the base material and conventionally welded joints. Eutectic components, including Mg-Si rich particles, were also observed, the distribution and morphology of these phase constituents influence the mechanical properties and behaviour of the processed joints.

Micro-hardness tests showed improved hardness values in FSP machined joints compared to conventionally welded joints. The optimized FSP parameters contributed to an improved hardness distribution, indicating increased strength and wear resistance in the machined joints [32].

The joining of **AA5083-H111** aluminium alloy-like plates was successfully achieved by both FSW and FSP methods. The joining efficiency reached 92% for FSW and 94% for FSP, indicating a strong and efficient bond [35].

In-depth analysis of the fractured surface of the specimens revealed the presence of a stepped formation at the end of the propagation stage. When comparing fatigue properties, it was observed that FSP performed better than FSW, with fatigue limit

values of 81 and 71, respectively, compared to the base metal fatigue limit of 87.

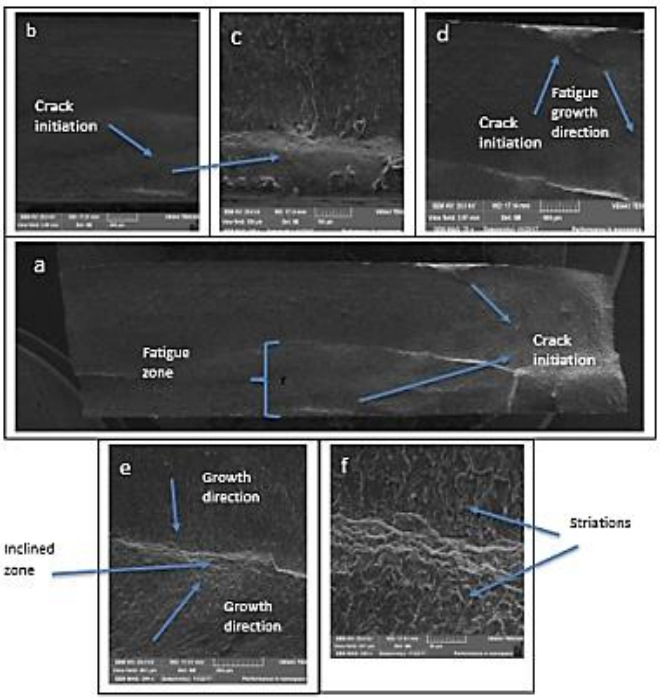

Figure 8. SEM fractography of FSP AA5083-H111 specimens for high load 110 MPa [33]

Fractographic analysis of fatigue failure surfaces indicated that some welds failed by cleavage failure, while in most cases, especially those with high joining efficiency, failure occurred in a ductile manner as can be seen in the figure 4. The dominant mechanism observed in the FS welds was coalescence of microvoids.

Additionally, the hardness of the FSW zone was found to be higher than that of the base metal, particularly in the case of alloy 5083-H111. This indicates a hardening effect resulting from the FSW process.

Overall, the findings demonstrate that both FSW and FSP techniques are capable of producing strong and reliable joints in AA5083-H111 aluminium alloys. Fatigue properties and fracture characteristics vary between the two methods, with FSP exhibiting closer performance to the base metal, while FSW shows some differences in fatigue behaviour and fracture types. [33].

In the case of Al7075 alloy where the plates are stacked microstructure changes, caused by the dynamic recrystallisation process, influence the mechanical properties of the material. FSP transformed the original material structure, which had an average grain size of 18 micrometers, into a uniform structure. This process resulted in the refinement of the structure down to grain sizes of approximately 8.2 and 12.1 micrometres for the overlapping regions in water and air respectively see, transition zones are generated between passes, as seen in the picture 8. These zones exist because transition zones are not processed twice. This was observed in an overlap process where the temperature of the specimen is reduced to room temperature before the next pass.

To evaluate the mechanical properties, tensile specimens oriented both parallel and perpendicular to the direction of travel of the FSP tool were fabricated. The results showed an improvement in yield strength, tensile strength and elongations of the specimens after FSP application.

Additionally, the Vickers hardness of the overlapped specimens increased compared to that of the original material after the application of the FSP process [33].

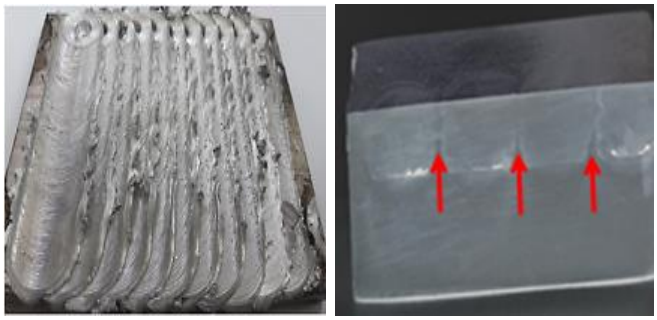

Figure 9. Overlap with macro structure of the overlapped region [34]

4. CONCLUSION

- The rotation speed during FSP significantly affects the microstructure and mechanical properties of the welded joints. Higher rotation speeds result in smoother surfaces, finer equiaxed grains in the Weld Nugget Zone (WNZ), and variations in hardness distribution. Increased rotation speeds also raise peak temperatures in the WNZ, influencing the distribution of precipitated phases;
- FSP induces noticeable changes in the microstructures of aluminium alloys, including refining, elimination of dendritic structures, decreased porosity and uniform particle dispersion. The process leads to a finer and more uniform grain size distribution compared to the base material, improving mechanical properties;
- The selection of cooling medium, such as air, underwater, or cryogenic, during FSP is crucial for achieving grain refinement and affecting the microstructural evolution and mechanical properties of aluminium alloys. Different cooling conditions can significantly influence the final properties of the processed material;
- Adjustment of process parameters, such as travel speed and applied pressure, can improve the

mechanical performance of aluminium alloys processed by FSP. Tensile strength and hardness of welded joints are influenced by microstructure, temperature distribution and the presence of surface defects, highlighting the importance of optimising these parameters for the desired mechanical properties.

- In the case of Al7075 alloy, FSP leads to the non-uniform transformation of the original material structure through dynamic recrystallization, producing a refined and uniform structure. Transition zones are generated between passes, having an impact on the grain size and overall material structure.

5. ACKNOWLEDGEMENTS

The paper has been developed within the project PN 23 37 01 02 entitle „Research on the modification of metallic materials properties using the innovative and environmentally friendly method of friction stir processing in liquid environment" (funded by the Ministry of Research, Innovation and Digitization within the Nucleu Program of ISIM Timisoara, contract 16N/2023 - Nucleu Program PN ISIM 2023-2026).

6. REFERENCES

1. Khedr, M., Hamada, A.W., *Review on the Solid-State Welding of Steels: Diffusion Bonding and Friction Stir Welding Processes*. Metals, 13, 54, (2023).
2. Akbari, M.; Parviz, A.; *A Review on Friction Stir Welding/Processing: Numerical Modeling*, Materials, 16, no. 17: 5890, (2023).
3. Mishra, R.S.; Ma, Z.Y.; *Friction stir welding and processing*. Mater. Sci. Eng. R Rep.,50, 1-78, (2005).
4. Akbari, M.; Ezzati, M.; *Investigation of the effect of tool probe profile on reinforced particles distribution using experimental and CEL approaches*. Int. J. Lightweight Mater. Manuf., 5, 213-223, (2022).
5. Das S.S.; Raja A.R.; Nautiyal H.; *A Review on Aluminum Matrix Composites Synthesized by FSP*. Macromol. Symp.,407, 2200119, (2023).
6. Papantoniou IG.; Markopoulos A.P.; Manolakos D.E.; *A New Approach in Surface Modification and Surface Hardening of Aluminum Alloys Using Friction Stir Process: Cu-Reinforced AA5083*. Materials; 13(6): 1278. https://doi.org/10.3390/ma13061278, (2020).
7. Glazoff, M.V.; Khvan, A.V.; Zolotorevsky V.S., *Structure and Microstructure of Aluminum Alloys in As-Cast State*. Cast. Aluminum Alloys, 133-234, (2019).
8. Mishra, R.S., Komarasamy, M.; *Friction Stir Welding of High Strength 7XXX Aluminum Alloys*. Elsevier Inc.: Amsterdam, The Netherlands, (2016).
9. Kissell, J.R., Ferry, R.L.; *Aluminum structures: A guide to their specifications and design*; John Wiley & Son Inc.: New York, NY, USA, (2002).
10. Sharma, V., Prakash, U.; *Microstructural and mechanical characteristics of AA2014/SiC surface composite fabricated by friction stir processing*, 4th International Conference on Materials Processing and Characterization, Materials Today Proceedings 2(4-5): 2666-2670, DOI: 10.1016/j.matpr.2015.07.229, (2015).
11. Cary Huang, L., He, L.; *Effects of non-isothermal aging on microstructure, mechanical properties and corrosion resistance of 2A14 aluminum alloy*. J. Alloys Compd., 842, 155542, (2020).
12. Wang, J.; Lu, Y.; *Effects of cooling condition on microstructural evolution and mechanical properties of friction stir processed 2A14 aluminum alloy*. Mater Res Express, (2021).
13. https://www.belmontmetals.com/product/a356-2-aluminum-alloy.
14. Akopyan, T.K.; Belov, N.A., *Characterization of structure and hardness at aging of the A319 type aluminum alloy with Sn trace addition*, Journal of Alloys and Compounds Volume 921, 15 November 2022, 166109, (2022).
15. Helzer, H.B.; *Modern welding technology*; Pearson/Prentice Hall: Upper New Jersey River, NJ, USA, (2005).
16. Mahoney, M.W.; Rhodes, C.G.; *Properties of friction-stir-welded 7075 T651 aluminum*. Met. Mater. Trans. A, 29, 1955-1964. (1998).
17. https://www.qdhcmetal.com/Aluminum-Sheet-and-Square/5083-H116-Aluminum-Plate.
18. https://matmatch.com/learn/material/7075-t6-aluminium.
19. Satyanarayana, MVNV.; Adepu, K.; *Influence of cooling media in achieving grain refinement of AA2014 alloy using friction stir processing*, Proc IMechE Part C: J Mechanical Engineering Science 0(0), Proceedings of the Institution of Mechanical Engineers Part C Journal of Mechanical Engineering Science 1989-1996 (vols 203-210) 234(22):095440622092285, DOI: 10.1177/0954406220922858, (2020).
20. Carvalho, C.J.; Lasecki, J.V.; *A Comparative Investigation on the High Temperature Fatigue of Three Cast Aluminum Alloys*. SAE Technical Papers, DOI: 10.4271/2004-01-1029, (2004).
21. Medlen, D.; Bolibruchová, D.; *Effect of Sb-Modification on the Microstructure and*

Mechanical Properties of Secondary Alloy 319, Archives of Metallurgy and Materials 61(2), (2016).
22. https://matmatch.com/learn/material/7075-t6-aluminium;
23. Anggono, A.D.; Widodo, T.; *Influence of tool rotation and welding speed on the friction stir welding of AA 1100 and AA 6061-T6*, Human-Dedicated Sustainable Product and Process Design: Materials, Resources, and Energy AIP Conf. Proc. 1977, 020054-1-020054-8, DOI: 10.1063/1.5042910, (2018).
24. Haifeng, Y.; Hongyun, Z.; *Effect of Stirring Pin Rotation Speed on Microstructure and Mechanical Properties of 2A14-T4 Alloy T-Joints Produced by Stationary Shoulder Friction Stir Welding*, Materials, 14, 1938. https://doi.org/10.3390/ma14081938, (2021).
25. Kouam, J.; Songmene, V.; *On chip formation during drilling of cast aluminum alloys*, Machining Science and Technology 17(2), DOI: 10.1080/10910344.2013.780546, (20213).
26. https://www.smithmetal.com/pdf/aluminium/2xxx/2014a.pdf.
27. Satyanarayana, K.A.; *Influence of cooling media in achieving grain refinement of AA2014 alloy using friction stir processing*, Proceedings of the Institution of Mechanical Engineers Part C Journal of Mechanical Engineering Science 1989-1996 (vol. 203-210) 234 (22), 095440622092285, DOI: 10.1177/0954406220922858, (2020).
28. Essam, M.; *Effect of Multi-Pass Friction Stir Processing on Mechanical Properties for AA2024/Al2O3 Nanocomposites*, Materials, 10, 1053; doi:10.3390/ma10091053; (2017).Saeidi, M.; Besharati Givi, M.K.; *Effect of Al2O3 nanoparticles on Microstructure and tensile strength of dissimilar friction stir welded Nanocomposite joint in AA7075 and AA5083 aluminum alloys*, 4th International Conference of Ultrafine Grained and Nanostructured Materials (UFGNSM2013), DOI: 10.13140/2.1.3248.0965, (2013).
29. Vipin, S.; Prakash, U., *Microstructural and mechanical characteristics of AA2014/SiC surface composite fabricated by friction stir processing*, Materials Today: Proceedings 2, 2666-2670, (2015);
30. Santella, M.L.; Engstrom, T.; *Effects of friction stir processing on mechanical properties of the cast aluminum alloys A319 and A356*, Scripta Materialia 53 201-206, (2005).
31. Kathiresan, G.; Ragunathan, S.; *Microstructural characterization of friction stir welded AA5083 aluminum alloy joints*, ITEGAM-JETIA, Manaus, v.9 n.43, p. 64-70, Sept./Oct., (2023).
32. Worood, H.; Mohsin, A.Al-S.; *Fatigue and Fracture Behaviours of FSW and FSP Joints of AA5083-H111 Aluminium Alloy*, IOP Conf. Series: Materials Science and Engineering 454 012055,doi:10.1088/1757-899X/454/1/012055, (2018).
33. Nourbakhsha, S.H.; Atrian, A.; *Effect of Submerged Multi-pass Friction Stir Process on the Mechanical and Microstructural Properties of Al7075 Alloy*, Journal of Stress Analysis, Vol. 2, No. 1, Spring-Summer, http://dx.doi.org/10.22084/jrstan.2017.14013.102. (2017).